OPTIMUM CONFIGURATIONS OF ANNULUS WITH TRIANGULAR FINS FOR LAMINAR CONVECTION

by

Zafar IQBAL[a*], Khalid Saifullah SYED[b], and Muhammad ISHAQ[c]

[a] Department of Mathematics, Government Emerson College, Multan, Pakistan
[b] CASPAM, Bahauddin Zakariya University, Multan, Pakistan
[c] Department of Computer Science, COMSATS Institute of Information Technology, Vehari, Pakistan

Original scientific paper
DOI:10.2298/TSCI130805139I

Optimum configurations of a finned annulus with longitudinal fins of triangular cross-section have been investigated numerically for the enhancement of overall (hydraulic and thermal) performance so that optimum use of energy and saving of cost may be achieved. A steady, laminar and incompressible flow is considered in the fully-developed region of the finned annulus subjected to the thermal boundary condition of constant heat transfer rate per unit axial length. Optimization has been carried out by using genetic algorithm. Finite element method is employed to perform the numerical simulation of the flow and provide function values to the optimizer. Using surface flow area goodness factor as the objective function, various optimum configurations have been proposed depending on practical and industrial requirements. A comparison of the present optimum configurations has been carried out with those based on the Nusselt number as an objective function. The results indicate that the present objective function gives, in many cases, cost- and weight-efficient optimum configurations with considerable reduction in pressure loss and provides optimum use of energy along with saving of the cost. Relative performance measures recommend the use of at least 18 fins to have trade off between the gain in heat transfer coefficient and loss in the pressure gradient.

Key words: *optimum configurations, genetic algorithm, laminar convection, finned double-pipe, finite element method, adaptive solution, hydraulic diameter*

Introduction

For promoting heat transfer rate in the thermal systems fins are widely used since long ago in various industrial fields such as petroleum and electronic industries, chemical processes, power plants, nuclear reactors, aerodynamics, *etc.* Because of their wide range of applicability in different disciplines and rapid increase in energy demand in all over the world, fins have attracted the attention of numerous researchers, and a vast literature has been devoted to their analysis. The use of fins in spite of its sole advantage of promoting heat transfer rate has many demerits in terms of requiring high pumping power, and increasing the weight and cost of the heat exchange system. It is natural to be interested in minimizing all these disadvantages while maximizing the benefit of enhanced heat transfer rate. Therefore, it is very crucial to use the fins judiciously. This poses a multi-objective optimization problem in which the shape and configu-

* Corresponding author, e-mail: zafariqbal176@hotmail.com

ration of the fins of a particular material are so chosen that maximize the heat transfer rate and minimize the weight, volume and cost of the fins and the pressure drop in the flow direction. The configuration of fins is determined by their number, height, and thickness. A good critical review may be found in [1, 2] on the optimization of extended surfaces.

In literature an inventory of the numerical and experimental work can be found for various types of longitudinally fins augmented internally/externally to the single/double pipes. Such types of finned ducts have been optimized by either optimizing the fin shape for specified geometry parameters [3-5], or by finding the optimum values of the configuration parameters for a given fin profile [6-9]. The detail of categorization of the problems and relevant literature review can be found in [2]. Rahmani *et al*. [10] presented different aspects of geometrical optimization for compact heat exchangers. For their studied flow they have shown the optimum tube layouts and ranges for the geometry parameters. Wang *et al*. [11] analyzed computationally the heat transfer and pressure drop performance of internally finned tubes with longitudinal wavy fins. They used Colburn *j*-factor as the measuring parameter and found that the overall heat transfer coefficient in wavy channel is higher than that in a plain fin channel with a larger loss of pressure drop. While the interrupted wavy fin tube could enhance heat transfer by 72-90%, with more than 2-4 times loss in the pressure drop. The sinusoidal wavy fin has the best area goodness factor among three different wavy fin patterns. Peng *et al*. [12] investigated the optimal design of plate-fin heat exchangers by using an improved particle swarm optimization algorithm. The thermal performance was measured by the Colburn *j*-factor. Their results show that the results computed by the proposed particle swarm optimization algorithm in their work are better than those in the preliminary design. The average rate of success is more than 80% which significantly higher. Ma *et al*. [13] performed the stress of internally finned bayonet tube in a high temperature heat exchanger. They studied the impact of gap between inner tube and inner fin on the stress and heat transfer performances. Their recommendation to the designers was that the inner fin and inner tube should not be welded together. Then Zeng *et al*. [14] studied the impact of fin different profiles on stress performance of internally finned tubes which are used in a high temperature heat exchanger. They considered three types of fin profiles, namely S-, V-, and Z-shape and found that the Z-shape has the best performance in terms of heat transfer and reliability, and recommended it for engineering application. Again they gave the recommendation for the designers that the inner fin and inner tube should not be welded together. There is need for the optimization of the gap width between the inner fins and the inner tube. The authors [10-14] used *j*-factor as the measuring parameter either for the analysis or for the optimization of their studies of different problems of finned surfaces under different flow conditions. However the heat transfer optimization of finned double pipe (FDP) is not a long listed work.

Syed [15] studied the effects of the fin and double pipe dimensions on the heat transfer and pressure loss for laminar convection in the FDP with longitudinal trapezoidal fins attached to the outer surface of the inner pipe. In [16, 17], the authors evaluated the performance of FDP in the entrance region of the developing flow for various configurations of the finned annulus. In [15-18] the authors studied the influence of the annulus configuration on the heat transfer coefficient and the pressure loss was studied for only finite sets of values of the configuration parameters. In the present work, we have investigated optimum configurations of the annulus by specifying the lower and upper bounds of the configuration parameters for the triangular fin profile. The surface flow area goodness factor has been employed as an objective function to be maximized in the optimization process. In [7-9] the authors investigated optimum configurations by considering the Nusselt number as an objective function. A comparison of the optimum configurations based on both of these objective functions has been given.

Problem formulation

Consider steady and laminar flow of viscous and incompressible fluid in the annulus of two concentric circular pipes with longitudinal fins augmented at the outer surface of the inner pipe, (fig. 1). The fins are straight, equally spaced, and non-porous with triangular cross-section and are made up of a highly conducting material. The flow is assumed to be fully developed. The thermal boundary conditions of constant heat transfer rate per unit axial length (H1 boundary conditions [19]) have been employed at the inner pipe of the finned annulus. If the inner pipe wall is assumed to be very thin with negligible thermal resistance, then the temperature variation in the wall fin assembly may be disregarded. Consequently the thermal boundary condition may be applied directly at the solid fluid interface. Further assumptions take the fluid to be Newtonian with constant properties and the flow with negligible viscous dissipation. Figure 2 shows the numerical solution domain in view of the symmetry of the geometry.

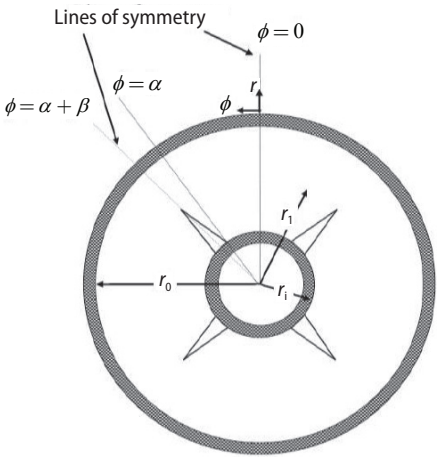

Figure 1. Cross-section of FDP

Momentum equation

Based on the assumptions, dimensionless form of the momentum equation of our governing the 2-D fluid motion is expressed:

$$\frac{1}{R}\frac{\partial U^*}{\partial R} + \frac{\partial^2 U^*}{\partial R^2} + \frac{1}{R^2}\frac{\partial^2 U^*}{\partial \phi^2} = \frac{-4}{C} \tag{1}$$

where

$$C = 1 - R_{\mathrm{m}}^2 + 2R_{\mathrm{m}}^2 \ln R_{\mathrm{m}} \tag{1a}$$

We have non-dimensionalized the previous equation by the following transformations:

$$U^* = \frac{U}{U_{\max}}, \quad R = \frac{r}{r_0} \tag{2}$$

Here

$$U_{\max} = -(1/4\mu)\frac{\mathrm{d}p}{\mathrm{d}z} r_0^2 \left\{1 - R_{\mathrm{m}}^2 + 2R_{\mathrm{m}}^2 \ln R_{\mathrm{m}}\right\} \quad \text{and} \quad R_{\mathrm{m}} = \frac{r_{\mathrm{m}}}{r_0} = \sqrt{1 - \frac{\hat{R}^2}{2\ln(1/\hat{R})}}$$

with $\hat{R} = r_i/r_{\mathrm{o}}$. The boundary conditions in their dimensionless form may can be expressed:
(a) At the solid boundaries I-III in fig. 2, no-slip conditions ensure that:

(i) $$U^* = 0 \text{ at } R = \hat{R}, 0 \le \phi \le \alpha \tag{3a}$$

(ii) $$U^* = 0 \text{ at } R = \frac{R_1 \hat{R}\sin\beta}{\hat{R}\sin(\phi - \alpha) - R_1 \sin(\phi - \alpha - \beta)} \text{ and } \alpha \le \phi \le \alpha + \beta \tag{3b}$$

(iii) $$U^* = 0 \text{ at } R = 1 \text{ and } 0 \le \phi \le \alpha + \beta \tag{3c}$$

(b) At the lines of symmetry IV-V in fig. 2, the symmetry conditions ensure that:

(iv) $$\frac{\partial U^*}{\partial \phi} = 0 \text{ at } \phi = 0 \text{ and } \hat{R} \le R \le 1 \tag{3d}$$

(v) $$\frac{\partial U^*}{\partial \phi} = 0 \text{ at } \phi = \alpha + \beta \quad \text{and } R_1 \le R \le 1 \tag{3e}$$

where $l^* = R_1 - \hat{R}$ is the actual fin height in dimensionless form in fig. 2.

Energy equation

Under the assumptions stated earlier regarding the nature of the fluid and that of its flow, convective heat transfer within the finned annulus may be modelled by the energy equation in its dimensionless form:

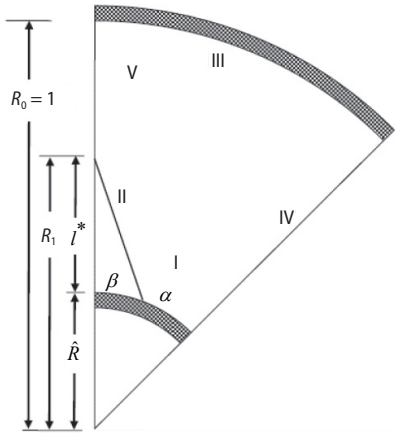

Figure 2. Numerical domain

$$\frac{\partial^2 \theta^*}{\partial R^2} + \frac{1}{R}\frac{\partial \theta^*}{\partial R} + \frac{1}{R^2}\frac{\partial^2 \theta^*}{\partial \phi^2} = \frac{U^*}{A_c^* \overline{U^*}} \tag{4}$$

where

$$\theta^*(r) = \frac{\theta(r,z) - \theta_w(z)}{\frac{\dot{Q}'}{\lambda_f}}$$

is the dimensionless temperature distribution, U^* – the dimensionless velocity distribution computed from eq. (1), and $\overline{U}^*$ – the average value of U^* over A_c^*, here A_c^* represents the free flow cross-sectional area in dimensionless form.

The computational domain shown in fig. 2 in which the energy eq. (4) is to be solved, subject to the following dimensionless boundary conditions.

(a) The boundary conditions of constant heat flux ensure that:

(i) $$\theta^* = 0 \quad \text{at} \quad R = \hat{R} \quad \text{and} \quad 0 \le \phi \le \alpha \tag{5a}$$

(ii) $$\theta^* = 0 \quad \text{at} \quad R = \frac{R_1 \hat{R} \sin\beta}{\hat{R}\sin(\phi - \alpha) - R_1 \sin(\phi - \alpha - \beta)} \quad \text{and} \quad \alpha \le \phi \le \alpha + \beta \tag{5b}$$

(b) At the outer pipe an adiabatic wall temperature condition ensures that:

(iii) $$\frac{\partial \theta^*}{\partial R} = 0 \quad \text{at} \quad R = 1 \quad \text{and} \quad 0 \le \phi \le \alpha + \beta \tag{5c}$$

(c) At the lines of symmetry the symmetry conditions ensure that:

(iv) $$\frac{\partial \theta^*}{\partial \phi} = 0 \quad \text{at} \quad \phi = 0 \quad \text{and} \quad \hat{R} \le R \le 1 \tag{5d}$$

(v) $$\frac{\partial \theta^*}{\partial \phi} = 0 \quad \text{at} \quad \phi = \alpha + \beta \quad \text{and} \quad R_1 \le R \le 1 \tag{5e}$$

Numerical solution

The finite element method (FEM) has been employed by using the MATLAB [20] routines for solving of the governing eqs. (1) and (4) subject to their respective boundary conditions. Adaptive *h*-refinement has been employed for highly accurate solutions. The FEM formulation of this governing system may be found in [7].

The adaptive solution has been obtained by employing the following steps: (1) Generate the initial triangulation mesh of the solution region. (2) Solve the equations on this mesh. (3) Compute the error estimation and test the stopping criterion. (4) Flag the triangles on the basis of this computed error estimation. (5) Refine the flagged triangles and obtain the refined mesh. (6) Compute the solution on the refined mesh. (7) Repeat steps (3-6) until stopping criterion is satisfied. For obtaining the adaptive solution we have applied the following relation for the error estimation (computed for each triangle) given by George [21]:

$$E(t) = A\left\| h^m (f - au) \right\|_t + B\left\{ \frac{1}{2} \sum_{e \in \partial t} h_e^{2m} \left[\vec{n}_e \left(c \nabla u_h \right) \right]^2 \right\}^{1/2}$$

where A, and B are weight indices both chosen as 0.15, m – the order parameter and is equal to 1 in the present work, $\vec{n}_e \left(c \nabla u_h \right)$ – the jump in flux across the element edge, h – the largest side length of the triangle, and h_e – the length of side e of the triangle.

If the error estimate defined previously exceeds from 0.5 then the refinement is made by flagging a triangle. Adaptation process is stopped when improvement in the $(\overline{f\mathrm{Re}})$ is less than 0.1%. Here $(\overline{f\mathrm{Re}})$ is the product of the Fanning friction factor and the Reynolds number averaged over the circumference of the cross-section. This criterion guarantees achievement of the property of grid independence solution. Moreover, as it is based on the shear stress, it renders appropriate mesh refinement for highly accurate calculation of the large velocity gradients in the boundary layer. Figure 3(a) shows the most refined mesh for the configuration determined by the parametric values $M = 15$, $H^* = 0.5$, $\beta = 3°$, and $\hat{R} = 0.5$. Due to very large velocity gradients at the fin-tip, highly refined mesh may be observed around it. Since percentage improvement can be calculated at the second and onward levels, therefore, the curves start from level 2. We note from the figure that ultimately the percentage improvement in $(\overline{f\mathrm{Re}})$ and $\overline{\mathrm{Nu}}$ become

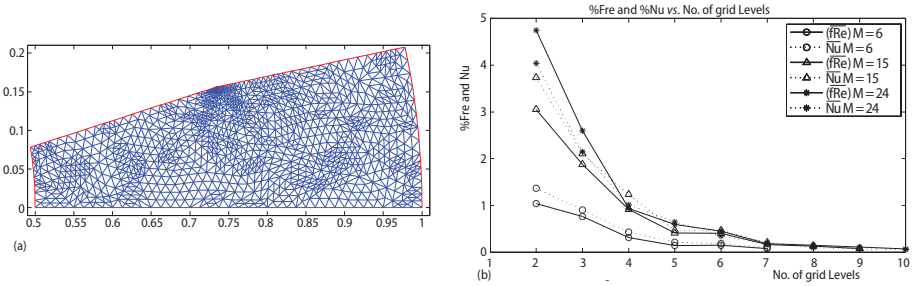

Figure 3. (a) Refined Mesh in the computational domain for the configuration determined by the parametric values $M = 15$, $H^* = 0.5$, $\beta = 3°$, and $\hat{R} = 0.5$ and (b) percentage improvement in $(\overline{f\mathrm{Re}})$ and $\overline{\mathrm{Nu}}$ plotted against grid levels for three different configurations

negligible for all the cases which reflect that the adaptation has been carried out up to the extent that makes the results grid independent. Moreover, for each case, the curves of $(\overline{f\mathrm{Re}})$ and $\overline{\mathrm{Nu}}$ overlap at certain grid level which indicates that the percentage improvements in $(\overline{f\mathrm{Re}})$ and $\overline{\mathrm{Nu}}$ become ultimately comparable. This is natural in convective heat transfer because the regions of large temperature gradients are also the regions of large velocity gradients with the converse being not necessarily true. Therefore, if the mesh is sufficiently refined to properly resolve the velocity gradients, the temperature gradients are also properly resolved. This is why it is sufficient to impose tolerance condition only on $(\overline{f\mathrm{Re}})$. The tolerance value 0.5 for $E(t)$ has been chosen heuristically through numerical experimentation. Smaller value of tolerance becomes too stringent and results into high computational cost while its large value may not give proper mesh resolution for sufficiently accurate determination of numerical results.

The numerical solution obtained by the previous procedure is employed for the evaluation of the objective function. Therefore, this procedure is invoked every time the optimizer requires the value of the objective function.

Optimization problem and its solution

When we consider the problem of optimizing FDP as a heat exchange system, we face the issue of appropriate choice of an objective function for optimum design of the finned annulus. If the sole objective is to achieve highest transfer coefficient irrespective of the rise in pressure loss, then usually Nusselt number is used as an objective function as has been done in the investigations [7-9]. However, if available pumping power is limited and pressure drop is of concern, then it is necessary to minimize fractional loss together with the maximization of Nusselt number. This poses a multi-objective optimization problem. However, there is an expression whose optimization involves maximization of Nusselt number and minimization of frictional loss. This is well-known surface flow area goodness factor widely used as a selection criterion for extended surfaces [10-14]. In the present work we employ this goodness factor to be the objective function and find optimum configuration of FDP. Here configuration means the number of the fins their height of the fin relative to the annular gap, fin-half-angle, and the annular gap of the pipes. Surface flow area goodness factor is defined as the ratio of Colburn j-factor and Fanning friction f and expressed as [22]:

$$j/f = \frac{\mathrm{Nu}\,\mathrm{Pr}^{-1/3}}{f\mathrm{Re}} \tag{6}$$

where Nu, Pr, and f are, respectively, the Nuesselt number, Prandlt number, and friction factor. The j/f based on the hydraulic diameter and averaged over the cross-section may be expressed:

$$(\overline{j/f})_h = \frac{\overline{\mathrm{Nu}_h}\,\mathrm{Pr}^{-1/3}}{(\overline{f\mathrm{Re}})_h} \tag{7}$$

The average Nusselt numbers, $\overline{\mathrm{Nu}_h}$, and the average product of Fanning friction factor and the Reynolds number, $(\overline{f\mathrm{Re}})_h$, may be expressed in its dimensionless form as [3-9, 15-18]:

$$\overline{\mathrm{Nu}_h} = \frac{D_h^*}{Ph_h^*\theta_b^*} \tag{8a}$$

$$(\overline{f\mathrm{Re}})_h = \frac{2D_h^{*2}}{C\overline{U}^*} \tag{8b}$$

The θ_b^* is the bulk mean temperature of the fluid in dimensionless form and is given by:

$$\theta_b^* = \frac{\iint_{A_c^*} U^* \theta^* \, dA_c^*}{\iint_{A_c^*} U^* \, dA_c^*} \tag{8c}$$

where C is constant given in eq. (1a) and D_h^* is dimensionless hydraulic diameter.

Parameters M, β, H^*, and $\hat{R}$ are subjected to fall between their lower and upper bounds. These bounds are determined by the extreme values of these parameters taken in this work, where $M \in \{3:3:30\}$, $\beta \in [0.5°,30°]$, $H^* \in [0.05,0.75]$, and $\hat{R} \in [0.05,0.75]$. Genetic algorithm has been used as an optimizer. It has been implemented by a computer code based on the function *ga* of MATLAB [20] optimization toolbox. The detailed description and implementation procedure of the optimizer may be found in [7].

Results and discussion

The numerical solution has been validated by comparing the present results obtained by the FEM with those given in [15] computed by the finite difference method. The comparison is excellent given in tab. 1.

We present our results in two subsections. In the first subsection we present and discuss the optimum configurations investigated in this study. In the second subsection we present performance evaluation of these optimum configurations using various performance measures and selection criteria.

Table 1. Comparison of the present results with the literature results for $H^* = 0.4$, 0.6, $\beta = 0°$, and $\hat{R} = 0.5$

H^*	M	$(\overline{j/f})_e$ [15]	$(\overline{j/f})_e$ present	H^*	M	$(\overline{j/f})_e$ [15]	$(\overline{j/f})_e$ present
0.4	6	0.3180	0.3178	0.6	6	0.3618	0.3616
	12	0.3135	0.3134		12	0.4058	0.4055
	18	0.2798	0.2797		18	0.3573	0.3569
	24	0.2488	0.2485		24	0.2908	0.2902
	30	0.2265	0.2264		30	0.2380	0.2373

Optimum configurations

In the first step, we investigated optimum values of the parameters which give maximum surface flow area goodness factor (maximum heat transfer rate and minimum frictional loss in the flow direction) $(j/f)_h$ defined by eq. (7). We denote the optimum values of M, H^*, $\hat{R}$, and β by M_{opt}, H^*_{opt}, $\hat{R}_{opt}$, and β_{opt}, respectively. When the surface flow area goodness factors $(j/f)_h$ is maximized, the optimum configuration is $M_{opt} = 3$, $H^*_{opt} = 0.05$, $\hat{R}_{opt} = 0.05$, $\beta_{opt} = 30°$, and $(\overline{j/f})_h = 0.6511$. We see that the lowest values of M, H^*, and $\hat{R}$ become their optimal values while for β, its highest value is the optimal value. This indicates that the optimum configuration is constituted by the smaller number of shorter and thicker fins attached to an inner pipe with very small radius. The reason for β being optimum at its upper bound appears to be that the lateral surface of fin is more effective in promoting the convection rate than the inner pipe surface because of which the optimizer maximizes the fin base angle in order to have maximum lateral surface area. There is in fact trade off between maximum free flow area, minimum heated perimeter and maximum convection (*i. e.* minimum bulk mean fluid temperature). Although this optimum fin configuration has the highest surface flow area goodness factor but owing to smaller surface area it may fail to fulfil industrial heat duty requirements. In addition, the inner pipe has very small radius that limits its heat carrying capacity and ability to uphold larger number of fins. This necessitates the optimization of $\hat{R}$, H^*, and β when M is specified.

Now we present optimization results for specified values of M in which H^*_{opt}, $\hat{R}_{opt}$, and β_{opt} have been investigated by maximizing $(\overline{j/f})_h$.

Figure 4 shows variation of H^*_{opt}, $\hat{R}_{opt}$, β_{opt}, and $(\overline{j/f})_h$ against M. We see that generally H^*_{opt} lies at its lower bound for all values of M. For $3 \le M \le 9$, $\hat{R}_{opt}$ lies at its lower bound while for higher values of M, $12 \le M \le 30$, it increases monotonically towards its upper bound. The fact that the optimum value of $\hat{R}$ increases with M is an attractive feature as a larger inner pipe is required to support a large number of fins for structural integrity. The β_{opt} decreases monotonically from its upper to the lower bound as the number fins increases from its smallest to largest value (M = 3 to 30).

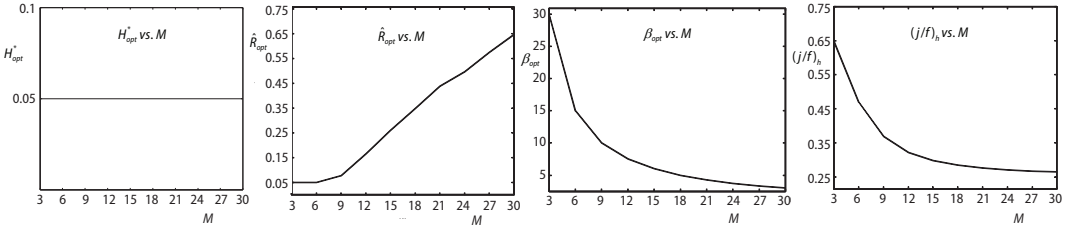

Figure 4. Optimum geometry parameters plotted against *M*

The $(\overline{j/f})_h$ depicts steep fall for $3 \le M \le 18$ and the fall becomes steady for higher values of M. There is a broader choice for the designer to select any number of fins out of the range $21 \le M \le 30$ for which the surface flow area goodness factor remains almost the same. For the case of specified values of the number of fins we may conclude that, if the number of fins is small then shortest and thickest fins on a narrow inner pipe will give maximum convection rate with minimum pressure loss and if the number of fins is large then shorter and thinner fins on a wider inner pipe will give larger surface flow area goodness factor. The β_{opt} decreases continuously as the number of fins increases. Moreover, if H^*_{opt}, $\hat{R}_{opt}$, and β_{opt} are to be used, then there will be no significant change in the surface flow area goodness factor by employing more than 18 fins.

We noted in the results presented in fig. 4 that H^*_{opt} for the maximization of $(\overline{j/f})_h$ lies at its lowest value and this is true for all values of M. These very small values of H^*_{opt} may not practically be useful. Therefore, we extend our investigation and find $\hat{R}_{opt}$ and β_{opt} when H^* and M are given and $(j/f)_h$ is the objective function.

Figure 5 gives the results of $(j/f)_h$ that have been maximized for specified values of H^* and M.

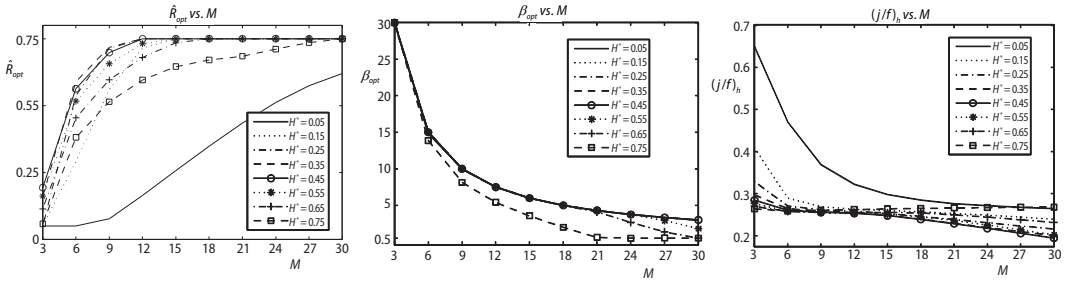

Figure 5. Optimum geometry parameters plotted against *M* when H^* is specified

We see that $\hat{R}_{opt}$ increases with M for all values of H^*, the rate of increase being dependent on the value of H^*. Except for the $\hat{R}_{opt}$-curve with smallest H^*, the optimum values of $\hat{R}$ first rise sharply with M and then asymptotically approach its upper bound at a value of M dependent on H^*. For a specified value of M in the range $3 \le M < 15$, $\hat{R}_{opt}$ first increases with H^* and after attaining a peak value at $H^* = 0.45$ for $M = 3$ and at $H^* = 0.35$ for all other values of M, it decreases with H^*. When M lies in the range $15 \le M < 27$, there is no significant influence of variation in H^* on $\hat{R}_{opt}$ in the range $0.15 \le H^* \le 0.65$. For $27 \le M \le 30$, only smallest value of H^* gives smaller $\hat{R}_{opt}$ while all other values of H^* give upper bound of $\hat{R}$ as its optimum value. This shows that for a specified value of fin height which is not too small, if we go on increasing the number of fins, only largest possible inner pipe will give optimum performance. The increasing trend of $\hat{R}_{opt}$ with M is advantageous from the design point of view as for the structural integrity larger inner pipe is required to support a large number of fins.

The β_{opt} decreases with M for all values of H^*, the rate of decrease being steeper for smaller values of M and steady for its larger values. The rate of decrease is particularly much steeper for very high fins. Moreover, β_{opt} does not show significant dependence on H^* that is not too large. These results are consistent with the physical nature of the problem as the fin thickness must be reduced with increase in the number of fins particularly for very high fins in order to provide sufficient free flow area for maximum convection and minimum pressure loss.

The curves of the surface flow area goodness factor $(\overline{j/f})_h$ *vs.* M show that, $(\overline{j/f})_h$ is decreasing with M for all values of H^* except $H^* = 0.75$ for which it starts rising insignificantly after reaching a minimum value. The optimum configurations for smallest fin height outperform those for other values of the fin height when $M \le 27$. But this fin height may not be practically useful in view of large heat duty requirement. The way $(\overline{j/f})_h$ varies with variation in the fin height depends on the number of fins. For smaller number of fins $3 \le \mathrm{M} \le 6$, $(\overline{j/f})_h$ decreases with H^*. For $M \ge 6$, the curves for larger fin height tend to over-ride those with smaller fin height depicting non-monotonic dependence of $(\overline{j/f})_h$ on H^*. However, for $6 \le M \le 15$, variation in $(\overline{j/f})_h$ with H^* except $H^* = 0.05$ is not significant. Therefore, any fin height may be chosen for this range of number of fins in view of design, cost and heat duty requirements. For $M \ge 15$, the curve of largest fin height tends to over-ride all other curves and ultimately for $M \ge 27$, largest fin height outperforms all other heights. This feature is very attractive in the situations where we need to employ very large heat transfer surface area in order to meet high heat duty requirement.

The results of the surface flow area goodness factor indicate that for smaller number of fins, shorter fins will give large surface flow area goodness factor while for large number of fins, higher fins will have to be employed for better performance.

In the present work we have investigated optimum configurations of the finned annulus on the basis of the surface flow area goodness factor, $\overline{j/f}$, which takes into account both hydraulic and thermal performance of the optimum configurations. Iqbal *et al.* [8] studied optimum configurations of the finned annulus on the basis of the Nusselt number which does not take into account their hydraulic performance. It would be interesting for a designer to have a comparison of the thermal and hydraulic performance of the optimum configurations based on both of these objective functions. Table 3 gives percenage change in the fin volume, friction factor, Nusselt number, and surface flow area goodness factor of the present optimum configuration relative to those given in [8].

Form tab. 3 we note that using $(\overline{j/f})_h$ as an objective function instead of $\overline{\mathrm{Nu}_h}$ we obtain reduction in the friction factor/pressure loss from 0.13% to 8.77% accompanied by the reduction in the heat transfer coefficient in the range 0% to 4.51%. Maximum reduction in

Table 3. Percent change in fin volume *V*, friction factor, Nusselt number, and surface flow area goodness factor of the present optimum configuration relative to those given in [8]

	M	3	6	9	12	15	18	21	24	27	30
% Change	*V*	6.98	–10.00	–48.00	–32.93	–21.76	1.60	25.49	12.82	31.25	22.92
	$(\overline{j/\mathrm{Re}})_h$	0.02	–0.13	–8.42	–7.83	–8.77	–1.15	–6.63	–4.05	–4.00	–2.28
	$\overline{\mathrm{Nu}_h}$	–0.09	0.00	–3.52	–4.26	–4.51	–0.17	–3.45	–2.78	–2.83	–1.71
	$(\overline{j/f})_h$	0.05	0.51	5.34	3.87	4.67	2.85	3.37	1.80	1.21	0.57

these quantities occurs for $M = 15$ and for $M = 21{:}3{:}30$, these reductions decrease to 2.28% and 1.71%, respectively. All the present optimum configurations give larger reduction in pressure loss than the corresponding reduction in heat transfer coefficient except that for $M = 3$. For the present objective function we observe gain in the surface flow area goodness factor for all values of M and this gain falls in the range 0.05% to 5.34%. The maximum value is achieved by the optimum configuration corresponding to $M = 9$. The results of the fin volume show that for $M = 6{:}3{:}15$ the optimum configurations based on the present objective function are significantly cost-and weight-efficient while for $M = 3$, $18{:}3{:}30$ those based on $\overline{\mathrm{Nu}_h}$ as an objective function are better in this regard.

Performance analysis of optimum configurations

In the present work we have investigated optimum configurations of a FDP rendering maximum surface flow area goodness factor. Although this goodness factor takes into account both the hydraulic and thermal performance, yet it is important to present separately the pressure drop and thermal performance analyses of the optimum configurations of the FDP relative to the un-FDP. For the case of specified pumping power, pressure drop in the fully developed region remains constant and is best represented by the Fanning friction factor in the form of its product with the Reynolds number. This product has been defined in eq. (8b).

Thermal performance analysis has been carried out in terms of the Nusselt number in the form its values relative to those for the corresponding un-FDP. Surface flow area goodness factor has also been presented relative to the corresponding un-finned geometry to evaluate the overall all performance of the FDP relative to the un-FDP.

Figure 6 presents these relative measures plotted against the number of fins for the corresponding optimum configurations. The results recommend the use of at least 18 fins with corresponding optimum values of the other parameters in order to have trade off between gain in the heat transfer coefficient and loss in the pressure gradient.

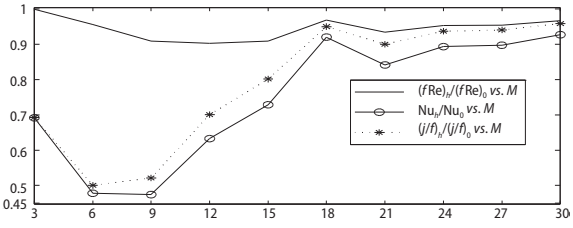

Figure 6. Relative friction factor, Nusselt number, and surface flow area goodness factor of optimum configurations plotted against the number of fins

Figure 7 presents all the relative performance measures for the optimum configurations corresponding to specified values of fin height and number of fins.

We note from the figure that relative friction factor decreases with M for all values of fin height H^* except its very small values $H^* = 0.05$, 0.15 for which it shows non-monotonic behavior. These trends are very encouraging in the sense that for a given pumping power the opti-

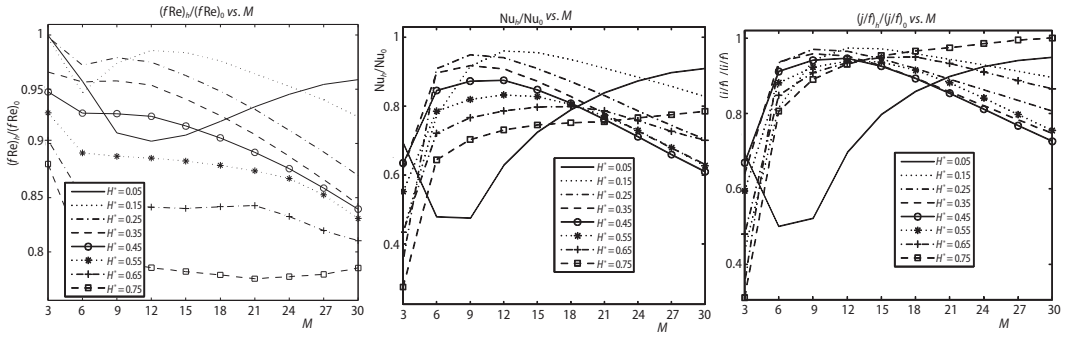

Figure 7. Relative friction factor, Nusselt number, and surface flow area goodness factor plotted against M for specific values of H^*

mum values of fin thickness and ratio of radii of inner and outer pipes do not let the frictional loss grow significantly for specified values of fin height and number of fins. Another interesting feature of the hydraulic performance is that except for $H^* = 0.05$, relative friction factor is higher for shorter fins and goes down as the fin height is decreased. The curves of the relative Nusselt number gain peaks at their respective values of M for specified values of H^* except $H^* = 0.05$, 0.75. For $H^* = 0.05$ the relative Nusselt number first falls down and then rises continuously with M while for $H^* = 0.75$ it rises steadily with M. This shows that only optimum configurations of lowest or highest fins improve their thermal performance with increase in M. No single fin height renders maximum relative Nusselt number for all values of the number of fins. In view of the results of relative Nusselt number shown in the figure an appropriate combination of the fin height and the number of fins will have to be chosen in order to gain maximum relative heat transfer coefficient. The results of the relative surface flow area goodness factor recommend the use of either smaller number of shorter fins or larger number of highest fins.

Conclusions

We have investigated optimum configurations of the triangular finned annulus of a double pipe for highly conducting wall-fin assembly. The design variables M, $\hat{R}$, H^*, and β have been optimized using surface flow area goodness factor as the objective function to be maximized under laminar flow conditions subjected to constant heat flux per unit length and uniform peripheral temperature boundary conditions. The performance of the investigated optimum configurations has been evaluated by the performance measures based on the pressure loss and the heat transfer coefficient. This study leads to the following conclusions.

- In the overall optimization, a smaller number of shorter and thicker fins on a very smaller inner pipe radius give maximum surface flow area goodness factor.
- For a specified number of fins, if the number of fins is small then shortest and thickest fins on a narrow inner pipe will give high convection rate with minimum pressure loss and if the number of fins is large then shorter and thinner fins on a wider inner pipe will give high surface flow area goodness factor. Moreover, if optimum parameters are to be used then there will be no significant change in the surface flow area goodness factor by employing more than 18 fins.
- When the number of fins and fin height both are specified, the results of surface flow area goodness factor indicate that for smaller number of fins, shorter fins will give large $\overline{(j/f)}_h$ while for large number of fins, higher fins will have to be employed for better performance.

- All the present optimum configurations in comparison with [8] give larger reduction in pressure loss than the corresponding reduction in the heat transfer coefficient for all values of number of the fins except $M = 3$. For the present objective function we observe gain in the surface flow area goodness factor for all values of M and this gain lies in the range 0.05% to 5.34%.
- For a specified number of fins, relative performance measures based on the hydraulic diameter recommend the use of at least 18 fins with corresponding optimum values of the other parameters in order to have trade off between gain in the heat transfer coefficient and loss in the pressure gradient.
- The results of the relative surface flow area goodness factor recommend the use of either smaller number of shorter fins or larger number of highest fins.
- A designer, by selecting the objective function of interest, may choose an optimum configuration of FDP from the present results in view of the cost, weight, structural integrity of the wall-fin assembly, and the heat duty. The proposed broad spectra of optimum configurations provide an optimum use of energy and handsome saving of cost.

Acknowledgement

Authors are thankful to the Higher Education Commission (HEC), Government of Pakistan, for its funding under the indigenous 5000 fellowship scheme.

Nomenclature

A – free flow area, [m^2]
D – diameter, [m]
$\mathrm{d}p/\mathrm{d}z$ – pressure gradient in finned geometry, [Pam^{-1}]
f – Fanning friction factor, [–]
H^* – fin height relative to the annulus, [–]
j/f – surface flow area goodness factor, [–]
l^* – actual fin height, [–]
Nu – Nusselt number, [–]
Pr – Prandtl number, [–]
Ph – heated perimeter, [m]
$\dot{Q}'$ – heat transfer rate per unit axial length of the pipe, [Wm^{-1}]
R – radial co-ordinate, [–]
Re – Reynolds number, [–]
$\hat{R}$ – ratio of the radii of the inner and outer pipes, [–]
R_1 – radial co-ordinate of the tip of the fin, [–]
R_m – radial position of the point of maximum velocity in the annulus without fins, [–]
r, ϕ, z – cylindrical co-ordinates
r_i – outer radius of the inner pipe, [m]
r_m – radial position of the point of maximum velocity, [m]
r_0 – inner radius of the outer pipe, [m]
U^* – axial velocity component, [–]
$U_{\max}$ – maximum axial fluid speed at a cross-section, [ms^{-1}]

Greek symbols

α – half-angle between successive fins, [rad]
β – fin half angle, [rad]
θ – temperature, [°C]
λ_f – thermal conductivity of the fluid, [Wm^{-1}K^{-1}]
μ – dynamic viscosity, [Pa·s]

Abbreviations

FDP – finned double pipe
FEM – finite element method
M – number of fins
V – fin volume

Subscripts

b – bulk
c – cross-section
e – equivalent diameter
h – hydraulic diameter
i – inner-pipe
0 – outer-pipe
opt – optimum value
w – solid wall

Superscripts

* – dimensionless quantity
$\bar{(\ )}$ – over bar, average value

References

[1] Razelos, P., A Critical Review of Extended Surface Heat Transfer, *Heat Transfer Engineering, 24* (2003), 6, pp. 11-28
[2] Gosselin, L., *et al*., Review of Utilization of Genetic Algorithms in Heat Transfer Problems, *International Journal of Heat and Mass Transfer, 52* (2009), 9-10, pp. 2169-2188
[3] Fabbri, G., Heat Transfer Optimization in Finned Annular Ducts under Laminar-Flow Conditions, *Heat Transfer Engineering, 19* (1998), 4, pp. 1521-1537
[4] Lan, C.-H., *et al*., Shape Design for Heat Conduction Problems Using Curvilinear Grid Generation, Conjugate Gradient, and Redistribution Methods, *Numerical Heat Transfer, Part A: Applications, 39* (2001), 5, pp. 487-510
[5] Hu, H., Chang, Y. P. M., Optimization of Finned Tubes for Heat Transfer in Laminar Flow, *Journal of Heat Transfer, 95* (1973), 3, pp. 332-338
[6] Zeitoun, O., Hegazy, A. S., Heat Transfer for Laminar Flow in Internally Finned Pipes with Different Fin Heights and Uniform Wall Temperature, *Heat Mass Transfer, 40* (2004), 3, pp. 253-259
[7] Syed, K. S., *et al*., Optimal Configuration of Finned Annulus in a Double Pipe with Fully Developed Laminar Flow, *Applied Thermal Engineering, 31* (2011), 8-9, pp. 1435-1446
[8] Iqbal, Z, *et al*., Optimization of Laminar Convection on the Shell-Side of Double Pipe with Triangular Fins, *Arabian Journal Science Engineering, 39* (2012), 3, 2307-2321
[9] Iqbal, Z., *et al*., Optimal Convective Heat Transfer in Double Pipe with Parabolic Fins, *International Journal of Heat and Mass Transfer, 54* (2011), 25-26, pp. 5415-5426
[10] Rahmani, R., *et al*., Different Aspects of Geometrical Optimization for Compact Heat Exchangers, *WSEAS Trnsactions on Applied and Theoretical Mechanics*, *2* (2007), 1, pp. 7-15 (patented by APU, UK, May 2001)
[11] Wang, Q. W., *et al*., Computational Analysis of Heat Transfer and Pressure Drop Performance for Internally Finned Tubes with Three Different Longitudinal Wavy Fins, *Heat Mass Transfer, 45* (2008), 2, pp.147-156
[12] Peng, H., *et al*., An Improved Particle Swarm Algorithm for Optimal Design of Plate-Fin Heat Exchangers, *Industrial & Engineering Chemistry Research, 49* (2010), 13, pp. 6144-6149
[13] Ma, T., *et al*., Stress Analysis of Internally Finned Bayonet Tube in a High Temperature Heat Exchanger, *Applied Thermal Engineering, 43* (2012), Oct., pp. 101-108
[14] Zeng, M., *et al*., Effect of Lateral Fin Profiles on Stress Performance of Internally Finned Tubes in a High Temperature Heat Exchanger, *Applied Thermal Engineering, 50* (2013), 1, pp. 886-895
[15] Syed, K. S., Simulation of Fluid Flow Through a Double-Pipe Heat Exchanger, Ph. D. thesis, University of Bradford, Bradford, UK, 1997
[16] Syed K. S,. *et al*., Convective Heat Transfer in the Thermal Entrance Region of Finned Double-Pipe, *Heat Mass Transfer*, 43 (2007), Mar., pp. 449-457
[17] Iqbal, M., Syed, K. S., Thermally Developing Flow in Finned Double-Pipe Heat Exchanger, *International Journal for Numerical Methods in Fluids*, 65 (2011), 10, pp. 1145-1159
[18] Syed, K. S., *et al*., Convective Heat Transfer in the Annulus Region of Triangular Finned Double-Pipe Heat Exchanger, *Computer and Fluid*, *44* (2011), pp. 43-55
[19] Shah, R. K., London, A. L., *Laminar Flow Forced Convection in Ducts*, Academic Press, London, 1978
[20] ***, MATLAB Version 7.13 (R2011b) Toolboxes, http://www.mathworks.com/help/techdoc/rn/bs1ef8o.html.
[21] George, P. L., *Automatic Mesh Generation Application to Finite Element Methods*, 1st ed., John Wiley and Sons, New York, USA, 1991
[22] Shah, R. K., Sekulić, D. P., Selection of Heat Exchangers and their Components, in: *Fundamentals of Heat Exchanger Design* (Ed. R. K. Shak), John Wiley and Sons, Inc., Hoboken, N.J., USA, 2007

Paper submitted: August 5, 2013
Paper revised: May 7, 2016
Paper accepted: June 8, 2016